JOURNAL OF BIOMEDICAL OPTICS 3(3), 227–236 (JULY 1998)

COMPENSATION OF EYE MOVEMENTS IN RETINAL SPECKLE FLOWMETRY USING FLEXIBLE CORRELATION ANALYSIS BASED ON THE SPECIFIC VARIANCE

Yoshihisa Aizu,[†] Toshimitsu Asakura,[†‡] and Atsushi Kojima*

[†]Muroran Institute of Technology, Department of Mechanical System Engineering, Muroran 050-8585, Japan; [‡]Hokkaido University, Research Institute for Electronic Science, Sapporo 060-0812, Japan; *Kowa Company Limited, Chofu Laboratory, Chofu-shi, Tokyo 182-0021, Japan

(Paper JBO/IB-005 received July 28, 1997; revised manuscript received Nov. 30, 1997; accepted for publication Jan. 12, 1998.)

ABSTRACT

Bio-speckle flowmetry using the photon correlation technique is useful for measuring the retinal blood flow velocity. In practical situations, however, it often suffers from eye-movement artifacts and other external moving factors. To solve this problem, we studied in this paper a flexible correlation analysis, by which the blood flow information can be effectively extracted from erroneous data influenced by displacement of the measuring point. The signal-analyzing system including the photon correlator directly stores the sequential counts of photoelectron pulses into a memory. After measurements, the stored data are read out and used to calculate the first-order statistics of time-integrated bio-speckles and the autocorrelation function with an arbitrary delay-time unit for an arbitrary period. These results are used to specify and to eliminate the erroneous parts of data due to the displacement of the measuring point. The usefulness of this technique was verified for a glass capillary model and human retinal vessels. © *1998 Society of Photo-Optical Instrumentation Engineers.* [S1083-3668(98)00203-2]

Keywords speckle; velocimetry; velocity measurement; speckle velocimeter; retinal blood flow; photon correlation.

1 INTRODUCTION

Bio-speckle fluctuations[1–7] can be widely observed from various living objects under illumination of the laser light, and applied to noninvasive metrological means for living dynamics of the objects. We have already reported bio-speckle flowmetry[8,9] that is useful for measuring the local blood flow velocity in human retinal vessels. Even though no absolute velocity can be obtained in this flowmetry, the measured values have consistent and stable linear characteristics with the mean blood flow velocity. The calibration process[9] using *in vitro* glass tubes gives a sense of the absolute velocity that is reliable and useful for practical uses.

In clinical applications, however, measurements for patients often suffer from eye-movement artifacts, involuntary body movements, and other unexpected events. The problem becomes more serious with diseased eyes because of the poor eye fixation. In bio-speckle flowmetry, the probe cross-sectional area is 20–50 μm in diameter while a typical vessel diameter to be explored is 50–150 μm. If the measuring point deviates with only 100 μm from the centerline of a retinal vessel, the measured data become readily erroneous and useless. There are several kinds of eye movements including voluntary and involuntary effects. We realized empirically that the bio-speckle method is troubled with flick- and drift-type small involuntary movements[10,11] and postural reflex movements (also involuntary), which easily cause the measuring point deviation of several ten to a hundred microns. In a laser Doppler velocimetric (LDV) system,[12] a special approach was employed to stabilize the measurements against eye movements. The LDV apparatus tracks the retinal vessel image in one dimension[13] or two.[14,15] This technique is promising for routine clinical uses. The same approach may be possible for bio-speckle flowmetry, but the electromechanical tracking system should be further refined because the sufficient performance for a tracking response is required for commercial apparatuses in the future.

Another solution may be to improve a signal processing method. This is easily performed and inexpensive, promising us reasonable results. This ap-

Address all correspondence to Yoshihisa Aizu. Tel: +81-143-47-3372; Fax: +81-143-47-3302; E-mail: aizu@muroran-it.ac.jp
T. Asakura's present address is: Faculty of Engineering, Hokkai-Gakuen University, Chuo-ku, Sapporo 064-0926, Japan.

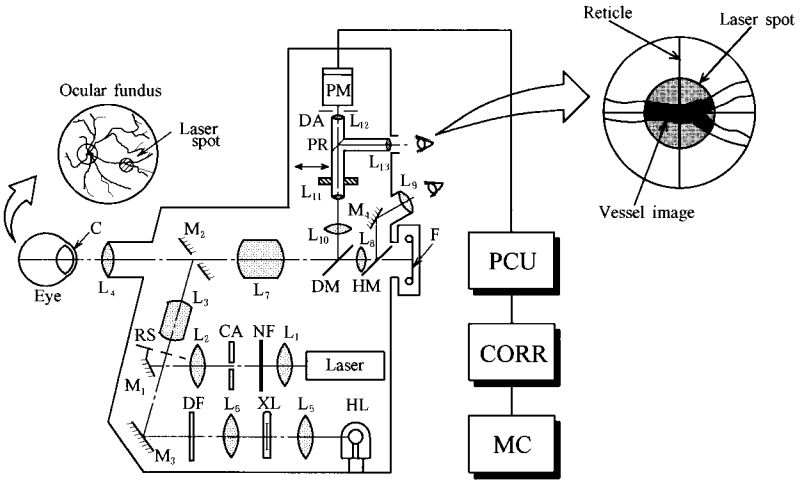

Fig. 1 Schematic diagram of the measuring apparatus.

proach is not exclusive but complementary to the use of the tracking system. Bio-speckle flowmetry employs the photon correlation technique,[16] which is useful for detecting an extremely small intensity of the scattered light from a human retina. A conventional correlation method yields directly an autocorrelation function through the total period of one measurement. If any eye movement occurs during the measurement, the resultant correlation function may be deteriorated, but cannot be corrected by an operator. When the error is identified, data will be discarded and the measurement must be repeated again. This may impose heavy tasks on a patient in usual clinical situations. We have already proposed[17] the improvement of correlation analysis for eliminating the effect of eye movements and discussed its usefulness from preliminary experiments. This paper reports a further experimental study on the improved correlation-analyzing method with both *in vitro* and *in vivo* experiments.

2 BIO-SPECKLE FLOWMETRY

Figure 1 shows a schematic diagram of the apparatus for measuring the retinal blood flow. The main optical system is provided by a standard fundus camera which was partly modified with a microscope (L_{11}, L_{12}, L_{13}, and PR), an X-Y microstage, a photomultiplier (PM), and a laser illumination system with a He-Ne laser source. A laser beam with the power of 40–80 μW illuminates a nearly 700-μm-diam area including a retinal vessel of interest. The intensity fluctuation of bio-speckles scattered by red blood cells in the retinal vessel is detected by the PM via a detecting aperture (DA) in the magnified image plane. The 400-μm-diam aperture and the 22.8× magnification define a nearly 20 μm probe cross-sectional area on the retinal vessel. The measuring position is defined by a reticule of eyepiece which optically corresponds to the center of the DA. Photoelectron pulses from the photomultiplier are counted in a photon counting unit (PCU) and fed into a photon correlator (CORR) which calculates an autocorrelation function of bio-speckle signals under the control of a microcomputer (MC). The present optical system has been more informatively described with the measuring principle in the previous papers.[8,9]

Red blood cells with a high flow velocity produce high frequency fluctuations of the speckle signal. The photon correlator treats the signal as the discrete pulse train and calculates the autocorrelation function in a digital manner. The resultant function is smoothed out and is used to evaluate the correlation time τ_c that is defined here as the delay time giving a half of the maximum correlation value at $\tau=0$. However, the correlation time may often be taken to be the time for the function to decrease to $1/e$. The above difference in the definition for the correlation time does not produce any significant problem in the study. We employed the former definition because of the simplicity for direct observations in measurements. The high frequency signal results in an early decay giving a small τ_c, thus giving a large value of the reciprocal of correlation time, $1/\tau_c$. On the other hand, a low flow velocity yields a slow decay having a small value of $1/\tau_c$. Our previous *in vitro* experiments[9] confirmed that the value $1/\tau_c$ has consistent linear characteristics with the mean flow velocity and that the calibration process gives us a sense of the absolute velocity. This is not a real absolute velocity but a velocity calibrated to the glass capillary model. Thus, the correlation analysis of bio-speckle fluctuations can be successfully utilized for measuring the retinal blood flow velocity.

As will be demonstrated later (for example, in Figure 7), a typical autocorrelation function obtained from a human retinal vessel shows an early decay to a nearly zero level, which is a typical curve for a major retinal blood vessel if no effect of eye

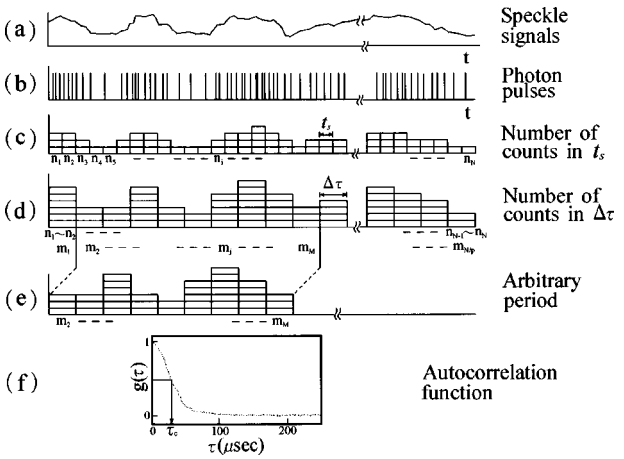

Fig. 2 Principle of the flexible correlation analysis.

movements is included. But the correlation function often shows a slow decay when the measuring point is located off the vessel by eye movements. This is probably due to a mixture of both high frequency fluctuations from the vessel and low frequency fluctuations from the tissue. No reliable velocity can be obtained from such a result. An operator must discard such erroneous data and repeat the same measurement until a desirable function is obtained. This process is impractical for clinical uses. However, the raw data which are used to compute the correlation function may still partly contain useful information about the retinal blood flow. If it is possible to extract only the useful part of data, erroneous results can be effectively utilized instead of being discarded. This is our motive for developing the flexible correlation analysis shown in this paper.

3 FLEXIBLE CORRELATION ANALYSIS

3.1 SYSTEM AND BASIC OPERATION

In order to eliminate the effect of eye-movement artifacts, we improved the signal-analyzing system which is based on the photon correlation technique. As already mentioned above, a basic concept for the improvement is to extract effectively the retinal blood flow information from erroneous photon counting data which are produced by eye movements. Figure 2 shows a principle of the signal analysis treated in this study. Speckle signals (a) are detected as a photoelectron pulse train (b), in which the number density of pulses is proportional to the speckle intensity. These pulses consist of signal components and dark current noise. Analysis of these pulses by means of a pulse height distribution[18,19] generally demonstrates that dark pulses are distributed in a lower range while signal pulses are in a larger range in their height. Thus, one can discriminate signal pulses from dark current pulses by using a certain threshold of the pulse height. This is done with a trigger level of the pulse generation in the discriminator which is a part of the photon counting unit. The resulting pulses are fed into a 256-channel digital photon correlator which is controlled by a personal computer. During one measurement time (run time), the signal pulses are counted every sampling time t_s which is variable, and the pulse counts in t_s, $n_1,n_2,\ldots,n_i,\ldots,n_N$ (c) are sequentially stored into the memory (RAM) via the pre-process unit in a real-time mode. Each of the data is counted in a 2- or 4-bit length, which is automatically selected by the correlator with respect to the ratio of the run time T and the sampling time t_s, because of a limit of the memory size. Successive four of 2-bit data or two of 4-bit data are converted to produce a single 8-bit data and, then, stored. If the detected light intensity is relatively high, a pulse count exceeds very often the bit length and an overflow may be detected. To avoid this trouble, the correlator is equipped with a pre-scale function which reduces the pulse count at a certain preset rate. The bit conversion and the pre-scale function are carried out in the pre-process unit of the correlator.

After a measurement, the stored data n_i ($i=1$–N) are read out from the memory, and are integrated in each time segment defined by $\Delta\tau$ which is set flexibly by an operator as pt_s ($p=$an integer). A schematic example in (d) corresponds to $\Delta\tau=2t_s$. The integrated pulse counts in $\Delta\tau$, $m_1,m_2,\ldots,m_j,\ldots,m_{N/p}$ (d) are, then, used to calculate the second-order autocorrelation function which is generally given by[20]

$$G^{(2)}(\tau)=\langle I(t)I(t+\tau)\rangle=\lim_{T\to\infty}\frac{1}{T}\int_{-T/2}^{T/2}I(t)I(t+\tau)dt, \tag{1}$$

where $I(t)$ is the speckle intensity detected at time t. The standard digital correlator[20,21] employs photoelectron pulse counts for computing the above function. Then, Eq. (1) may be expressed in a discrete form, which is actually computed in our system, as follows:

$$G^{(2)}=G^{(2)}(q\Delta\tau)=\sum_{j=1}^{N/p}m_jm_{j+q}, \tag{2}$$

where q is an integer giving the channel number (1–256 in our system), and N/p is the total number of terms in the summations. Let the fluctuations of pulse counts from the average counts $\langle m\rangle$ in $\Delta\tau$ be expressed by $\Delta m=m-\langle m\rangle$. Then, Eq. (2) is rewritten as

$$G^{(2)}(q\Delta\tau)=\frac{N}{p}\langle m\rangle^2+\sum_{j=1}^{N/p}\Delta m_j\Delta m_{j+q}. \tag{3}$$

The second term in Eq. (3) indicates a correlation of the pulse count fluctuations, which is referred to as an autocovariance $C(q\Delta\tau)$ (Ref. 22) and is given by

$$C(q\Delta\tau)=\sum_{j=1}^{N/p}\Delta m_j\Delta m_{j+q}=G^{(2)}(q\Delta\tau)-\frac{N}{p}\langle m\rangle^2. \tag{4}$$

Since the fluctuation component is the quantity of interest here, the personal computer finally displays the plot of $C(q\Delta\tau)$ in a normalized form as

$$g(\tau)=\frac{C(q\Delta\tau)}{C(0)}. \tag{5}$$

Finally, the correlation time τ_c is evaluated for the function $g(\tau)$ as shown in (f) of Figure 2.

In this analysis, the time segment $\Delta\tau$ corresponds to a unit of the delay time of the autocorrelation function. The aim of the integration $\Delta\tau=pt_s$ is to change a unit delay time or a full-scale range of the delay time for the 256-channel correlator. Let us take a simple example of the sampling time $t_s=1$ μs, $p=1$ and, then, $\Delta\tau=1$ μs. A calculated correlation function has a delay-time resolution or unit of 1 μs in the full-scale range up to 256 μs. When we calculate a correlation function of some signals which have the correlation time τ_c longer than 256 μs, the resultant curve may show a quite slow decay and become unavailable for determining τ_c in this full-scale range. The problem is easily solved by enlarging a full scale of the delay time such as to 512 or 768 μs, which is done by taking $p=2$ or 3. Since the raw data of sequential pulse counts, n_i, are stored in the memory, an operator is able to repeat without the limit the calculations with different $\Delta\tau$'s. To measure properly the correlation time τ_c, we recommend that the delay time unit $\Delta\tau$ may be so adjusted that the correlation time or the time needed for the correlation function $g(\tau)$ to drop to the half would be roughly in the delay time range of 50–100 channels (or $\Delta\tau$ times 50–100). After some trials, the correlation function may properly be evaluated in this way. A change of the unit delay time or the full-scale range can also be made by varying the sampling time t_s when counting photoelectron pulses, since the sampling time is also variable in our correlator. But an operator has to perform another measurement with a new sampling time. Therefore, the operation of $\Delta\tau=pt_s$ is quite convenient for practical uses. It should be noticed, however, that the above integration generally causes high frequency signals to be smoothed out if a relatively large $\Delta\tau$ is employed, because it works as a low-pass filter. As mentioned above, the value of $\Delta\tau$ may be limited to a time range much smaller than the correlation time τ_c of signals to be measured for the retinal blood flow. Our experience may give the range of $\Delta\tau$ to be usually about 0.5–3 μs with which the calculated correlation functions safely provide us the blood flow information. It is also possible, if necessary, to use only a limited time region of the sequential data m_j for calculating the correlation function. Figure 2(e) demonstrates

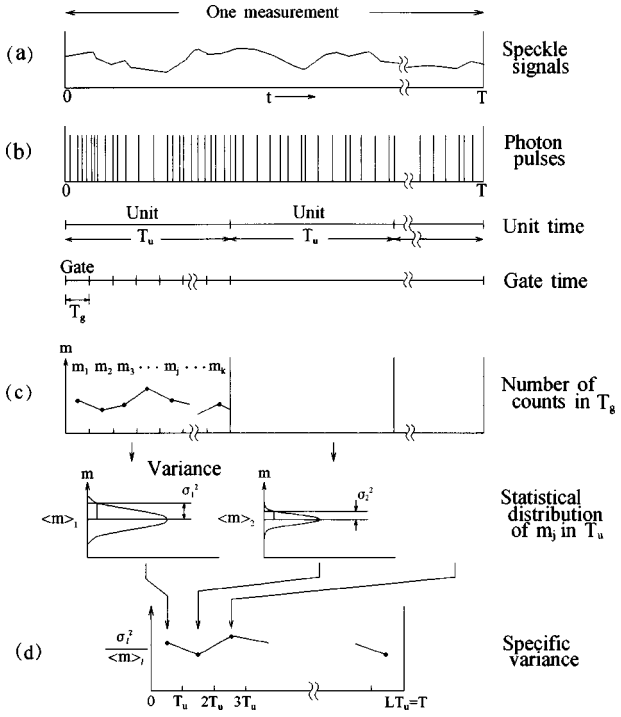

Fig. 3 Process for estimating the specific variance.

an example of the region of $m_2\sim m_M$. This operation is useful for the time-division correlation analysis as will be shown in Figure 8 of Sec. 4.2. The computer may also print them out and save them in a magneto-optic disk MO. The raw stored data n_i ($i=1$–N) in the memory can also be saved into the MO optionally.

3.2 SPECIFIC VARIANCE

Eye movements lead to the displacement of a measuring point from the vessel center to the surrounding tissue, and cause an error to the measured results. This defect may be reduced by means of the flexible correlation analysis. But there is one more problem how one finds out or discriminates erroneous parts from the data for the total run time stored in the memory. To solve this problem, we employed a certain criterion using the specific variance which is estimated on the basis of the first-order temporal statistics of time-integrated bio-speckle fluctuations.[7,23] Figure 3 schematically describes a method for estimating the specific variance. This estimation may be made before calculating the correlation function. The memory stores sequential pulse count data n_i ($i=1$–N) for a period of the run time T ($T=Nt_s$). The period T is divided by a subperiod T_u which is referred to as a unit time here, and totally $L(=T/T_u)$ numbers of units are produced. The pulse count data are read out from the memory and are integrated in each gate time T_g instead of the delay-time unit $\Delta\tau$. Thus, T_g is different from the delay-time unit $\Delta\tau$ shown in Figure 2. Note that T_g is employed for smoothing out high frequency

components as a low-pass filter, while $\Delta\tau$ is used for changing the delay time unit with the high frequency components being kept. The gate time T_g is preset as $T_g = T_u / k$ (k = an integer). Thus, the system has k numbers of sequential integrated pulse counts, $m_1, m_2, \ldots, m_k$ for each unit time T_u as shown in Figure 3(c). Then, an average number $\langle m \rangle_l$ and a variance σ_l^2 of the integrated counts are calculated for a lth unit as

$$\langle m \rangle_l = \frac{1}{k} \sum_{j=1}^{k} m_j \tag{6}$$

and

$$\sigma_l^2 = \frac{1}{k} \sum_{j=1}^{k} \{m_j - \langle m \rangle_l\}^2 = \langle \Delta m^2 \rangle_l , \tag{7}$$

where l is a unit number and takes an integer of $1-L$. The specific variance is obtained by their ratio for each unit time T_u as

$$\frac{\sigma_l^2}{\langle m \rangle_l}. \tag{8}$$

In the speckle theory,[24] the first-order spatial statistics of speckle intensity patterns yield a contrast which is expressed by

$$\frac{\sigma_I}{\langle I \rangle}, \tag{9}$$

where σ_I and $\langle I \rangle$ are the standard deviation and the ensemble average of speckle intensity patterns. If the speckle pattern moves with a constant speed but without changing its intensity distribution, a point detector may produce the corresponding temporal speckle signal $I(t)$. A ratio of the standard deviation to the average intensity of the signal $I(t)$ also gives a value of the ''contrast'' equivalent to Eq. (9). According to this analogy between the spatial and temporal statistics, it may be possible with the assumption of ergodicity[22] to consider a ''contrast'' here for the integrated pulse counts m which is given by

$$\frac{\sigma_l}{\langle m \rangle_l}. \tag{10}$$

Thus, it may be noticed that the specific variance in Eq. (8) closely resembles the ''contrast'' in Eq. (10), although Eq. (8) employs the variance instead of the standard deviation. Finally, a temporal change of the specific variance can be estimated as shown in Figure 3(d).

Figure 4 shows a concept of the data discrimination by using the specific variance. Speckle signals obtained from a retinal vessel have high frequency fluctuations while those from the surrounding tissue contain low frequency fluctuations, as shown in (a). By integrating the sequential pulse count data

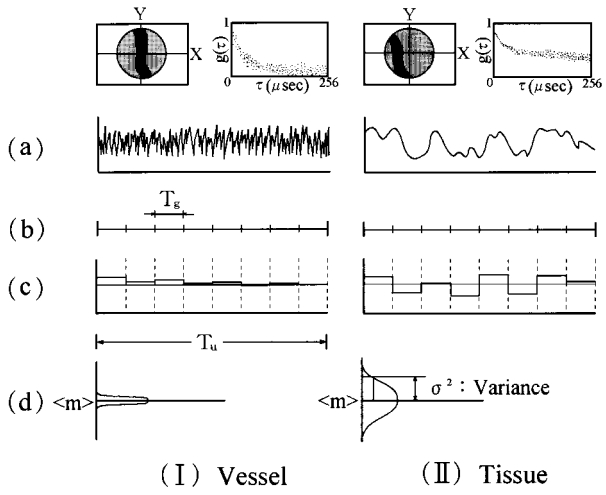

Fig. 4 Data discrimination using the specific variance.

over the preset gate time T_g, the result for the vessel becomes rather smoothed, but some fluctuations still remain in the result for the tissue as shown in (c). A statistical distribution of the integrated counts in the unit time T_u becomes narrow for the vessel and broad for the tissue as shown in (d). This difference can be evaluated by the specific variance $\sigma_l^2 / \langle m \rangle_l$ which takes a small value for the vessel and a large one for the tissue. Thus, we can discriminate the data segments for the vessel from those for the tissue and use only the former for calculating a correlation function.

In order to make effective use of the specific variance, the gate time T_g should be determined properly by considering the nature of the specific variance. Let us consider the case that the gate time increases from T_g to $T_g' = hT_g$ (h is an integer). The discussion here is applied to a certain unit such as lth, but the subscript $\{l\}$ is omitted below for simplicity. With $T_g' = hT_g$, this unit contains $k' = k/h$ numbers of sequential integrated pulse counts, $m_1', m_2', \ldots, m_k'$, where

$$m_s' = \sum_{j=(s-1)h+1}^{sh} m_j = m_{(s-1)h+1} + m_{(s-1)h+2} + \cdots + m_{sh} \tag{11}$$

with $s = 1 \sim k'$. The average number $\langle m' \rangle$ in this case is expressed as

$$\langle m' \rangle = \frac{1}{k'} \sum_{s=1}^{k'} m_s' = \frac{1}{k'} \sum_{j=1}^{k} m_j = h \langle m \rangle. \tag{12}$$

The specific variance is written by using Eqs. (11) and (12) as

$$\sigma'^2=\langle \Delta m'^2\rangle$$
$$=\frac{1}{k'}\sum_{s=1}^{k'}\{m'_s-\langle m'\rangle\}^2$$
$$=\frac{1}{k'}\sum_{s=1}^{k'}\{\Delta m_{(s-1)h+1}+\Delta m_{(s-1)h+2}+\cdots+\Delta m_{sh}\}^2$$
$$=\frac{1}{k'}\sum_{s=1}^{k'}\left[\sum_{x=1}^{h}\Delta m^2_{(s-1)h+x}+2\sum_{y=1}^{h-1}\sum_{x=1}^{h-y}\{\Delta m_{(s-1)h+x}\cdot\Delta m_{(s-1)h+x+y}\}\right]$$
$$=\sum_{x=1}^{h}\langle \Delta m_x^2\rangle+2\sum_{y=1}^{h-1}\sum_{x=1}^{h-y}\langle \Delta m_x\cdot\Delta m_{x+y}\rangle. \quad (13)$$

The first term of the last expression in Eq. (13) may be approximated, with a large number of statistical samples, to be

$$\sum_{x=1}^{h}\langle \Delta m_x^2\rangle\cong h\langle \Delta m^2\rangle. \quad (14)$$

The second term indicates the summations of all the correlation values of fluctuation components $\Delta m = m-\langle m\rangle$ between any two of h terms which are summed up over the increased gate time $T'_g=hT_g$ and, thus, shows the effect of integration or smoothing out. This can be discussed for the three typical cases in the following.

(1) When the speckle signals $I(t)$ or photon pulse counts n_i have high frequency fluctuations or the short correlation time such as $\tau_c \ll hT_g$, Δm_x has almost no correlation with Δm_{x+y}. Thus, we have

$$\langle \Delta m_x\cdot\Delta m_{x+y}\rangle\approx 0. \quad (15)$$

Substitution of Eq. (15) into Eq. (13) gives the following results, by using Eqs. (7), (12), and (14), as

$$\frac{\sigma'}{\langle m'\rangle}=\frac{1}{\sqrt{h}}\cdot\frac{\sigma}{\langle m\rangle} \quad (16)$$

and

$$\frac{\sigma'^2}{\langle m'\rangle}=\frac{\sigma^2}{\langle m\rangle}. \quad (17)$$

This means that the temporal signal contrast decreases by $1/\sqrt{h}$ with an increase of the gate time by a factor h, but the specific variance does not change.

(2) In the case of low frequency signals with the long correlation time as $\tau_c \gg hT_g$, Δm_x may be highly correlated with Δm_{x+y}. Then,

$$\langle \Delta m_x\cdot\Delta m_{x+y}\rangle\approx\langle \Delta m^2\rangle \quad (18)$$

and

$$\sigma'^2\approx h\langle \Delta m^2\rangle+h(h-1)\langle \Delta m^2\rangle=h^2\sigma^2. \quad (19)$$

This yields simply the following results:

$$\frac{\sigma'}{\langle m'\rangle}=\frac{\sigma}{\langle m\rangle} \quad (20)$$

and

$$\frac{\sigma'^2}{\langle m'\rangle}=h\,\frac{\sigma^2}{\langle m\rangle}, \quad (21)$$

which indicate that the temporal signal contrast has no change, but the specific variance increases by h with an increase of the gate time by h.

(3) If the signal frequency or the correlation time is in a medium range between the cases (1) and (2), the relations may be expressed as

$$0<\langle \Delta m_x\cdot\Delta m_{x+y}\rangle<\langle \Delta m^2\rangle \quad (22)$$

and

$$h\sigma^2<\sigma'^2<h^2\sigma^2. \quad (23)$$

Thus, $\sigma'/\langle m'\rangle$ and $\sigma'^2/\langle m'\rangle$ also take some medium values between the cases (1) and (2). This means that the temporal signal contrast decreases and the specific variance increases, both in a moderate manner.

These cases (1) to (3) are summarized in Table 1.

Table 1 Comparison of $\sigma/\langle m\rangle$ and $\sigma^2/\langle m\rangle$ for increasing gate time T_g by a factor h.

Speckle fluctuation	High freq.	Medium freq.	Low freq.
Correlation time	$\tau_c \ll hT_g$	$\tau_c \lesssim hT_g$	$hT_g \ll \tau_c$
$\sigma/\langle m\rangle$	$1/\sqrt{h}$	$1/\sqrt{h}<$ factor <1	1
$\sigma^2/\langle m\rangle$	1	$1<$ factor $<h$	h
$K=\langle \Delta m_x\cdot\Delta m_{x+y}\rangle$	$\fallingdotseq 0$	$0<K<\langle \Delta m^2\rangle$	$\fallingdotseq\langle \Delta m^2\rangle$
Case in Sec. 3.2	(1)	(3)	(2)

The above analysis shows that the specific variance may be constant for the vessel and increases for the tissue when the gate time T_g is increased in a schematic example of Figure 4. Thus, the gate time T_g may be determined in such a way that the specific variance shows a sufficient separation between the values for the vessel and tissue. However, the above discussion with Table 1 indicates two possibilities for our purpose, that is to say, $\sigma/\langle m\rangle$ and $\sigma^2/\langle m\rangle$. The temporal signal contrast $\sigma/\langle m\rangle$ is actually a very popular dimensionless measure and easy to understand its physical meaning. However, the primary interest in this study is to extract information about the retinal blood flow

from erroneous data that are produced by a mixture of unknown low frequency components. To discriminate the data for the vessel from those for the tissue with unknown low frequency fluctuations, different values of the gate time T_g should be used by way of trial. Table 1 means that the specific variance for the vessel may keep a constant value even if the gate time T_g varies but the contrast may decrease. Once a threshold is fixed to be a value somewhat larger than the specific variance for the vessel, it is not necessary for the threshold to be changed even when the gate time T_g is varied according to unknown low frequency fluctuations that are variable in the tissue. This can be practically quite useful. But the use of the temporal signal contrast requires a proper adjustment of the threshold every time for a change of the gate time T_g. By this reason, we employed the specific variance in this study, although it is an unfamiliar physical value.

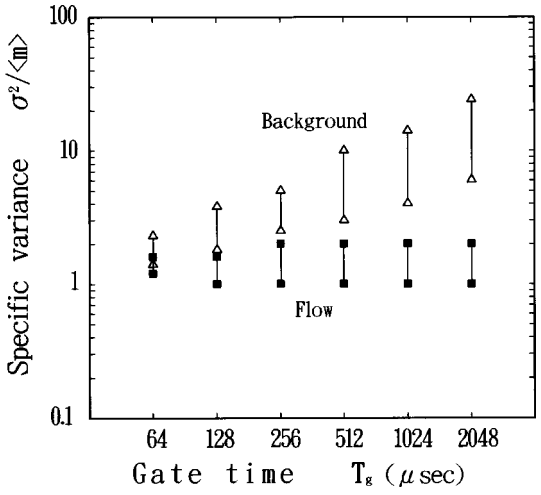

Fig. 5 Ranges of the specific variance obtained experimentally with various gate times for the flow and the background.

4 EXPERIMENTS

4.1 *IN VITRO* MEASUREMENTS

To verify the ability of the flexible correlation analysis for reducing the effect of eye movements, we first carried out *in vitro* experiments using a simple eye model. This model consists of a pupil of 7-mm-diam aperture, a 18 mm focal length lens, a 150-μm-diam glass capillary containing a flow of human blood, and a background cell having 1-μm-diam acrylic particles suspended in water. The capillary is placed at the focal distance backward from the lens and in front of the background. The whole model is fixed on a translation stage controlled by a computer, with which a measuring point can be displaced with a constant speed during a measurement. The blood flow velocity in the capillary was regulated by the level difference between two containers in order to change the correlation time τ_c of speckle fluctuations.

The first experiment was performed to investigate a change of the specific variance $\sigma^2/\langle m\rangle$ with various values of the gate time T_g for the photon count data obtained in the flow and the background. The sampling time t_s and the unit time T_u were set to be 1 μs and 65.5 ms, respectively. A flow velocity in the capillary and a particle concentration in the background cell were carefully adjusted in such a way that their speckle fluctuations should have nearly 30 and 440 μs, respectively, in a correlation time τ_c. These values were determined empirically on the basis of our previous observation for human volunteers in which typical values of the correlation time τ_c ranged from 20 to 100 μs for vessels and from 300 to 700 μs for tissues. Figure 5 shows ranges of the specific variance obtained experimentally as a function of the gate time T_g. As expected theoretically in Sec. 3.2, the specific variance gives a nearly constant value for the flow and becomes large with an increase of the gate time. A short gate time is insufficient for integrating or smoothing the count data of the flow and, thus, the remaining fluctuations yield a value of the specific variance close to that for the background. A good separation is obtained with $T_g = 512$ μs or longer.

It should be noticed that a condition of the separation in Figure 5 is governed by the correlation time (or frequency components) of bio-speckle fluctuations both for the flow and the background. Our discrimination method assumes that a clear difference in the correlation time exists between the retinal vessel and the surrounding tissue. A small difference may fall in confusion of these results for the flow and the background. We, then, investigated the separation between the specific variances for the background with $\tau_c = 440$ μs and the flow with different correlation times varying in $\tau_c = 30$–90 μs. The values of t_s and T_u were fixed to be the same as Figure 5, while the gate time T_g was set to be 1 or 2 ms. Although the results are not shown here, the specific variance for the flow with $\tau_c = 90$ μs was close to that for the background, but a situation of the separation was somewhat improved with a longer gate time. By assuming a criterion of $\sigma^2/\langle m\rangle = 8.5$ for the discrimination, the rate of misreading was evaluated to be 6.3% and 9.7% for the flow and the background, respectively. From this experiment, a difference of four times may be desired, for reliable discrimination, between the correlation times for the flow and the background.

Next we measured temporal variations of the specific variance for displacement of the eye model during a measurement for 4.2 s. Four different values of the gate time $T_g = 256$, 512, 1024, and 2048 μs were employed, while the sampling time t_s and the unit time T_u were fixed to be 1 μs and 131 ms, respectively. The measuring point was first set on the background in the left hand side of the capillary

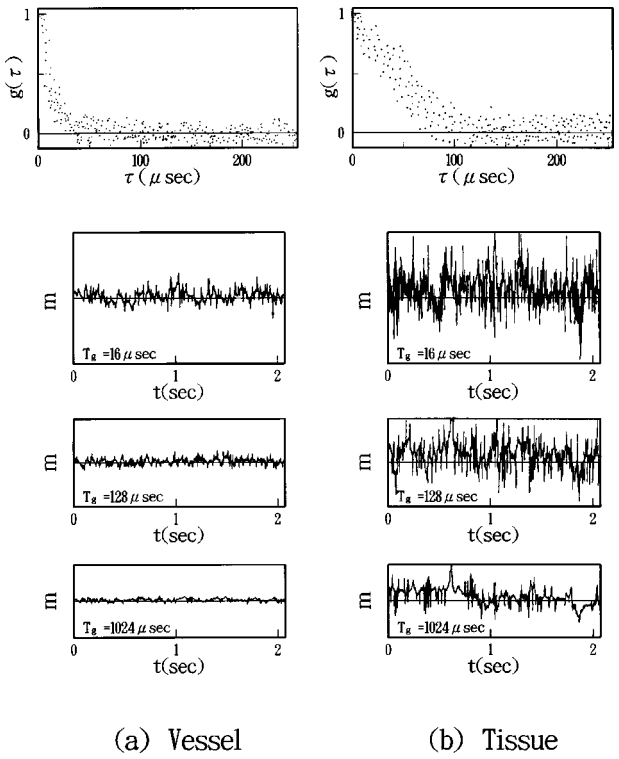

Fig. 6 Correlation functions, and direct plots of the integrated count data m.

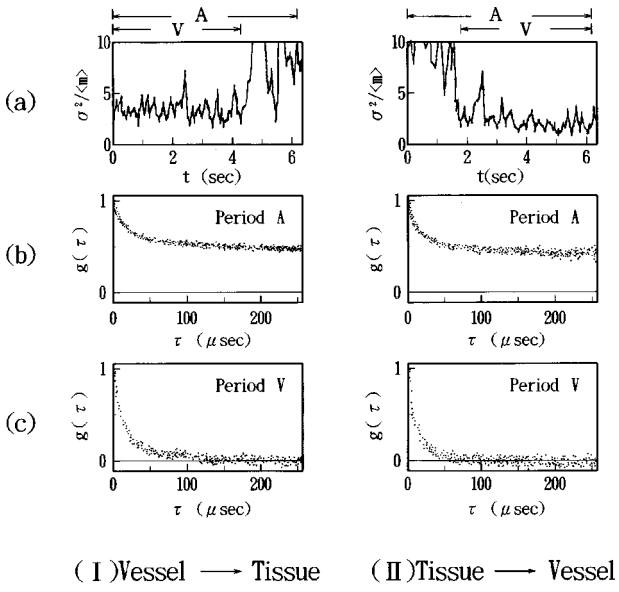

Fig. 7 Temporal recordings of the specific variance and the corresponding correlation functions.

and, then, moved to the right with the constant speed of 60 μm/s, crossing the capillary. We verified that the specific variance was large in the beginning, became small in the capillary taking values of 1–2, and then increased again. A change of the specific variance measured almost agreed with the visual observation of actual displacement. A better separation between the flow and the background was again obtained with a longer gate time. If one selects only the time region giving a small specific variance, then a desirable correlation function may be calculated. A criterion value in the specific variance should be carefully determined for reliable discrimination.

4.2 *IN VIVO* MEASUREMENTS

We next carried out some measurements on human retina in order to confirm the usefulness of our flexible correlation analysis for the *in vivo* condition. The general measuring conditions used in the apparatus of Figure 1 were the same as those described in the previous paper.[9] Volunteers were asked to fixate on the target installed in the apparatus. Then, an operator was able to locate the measuring point on or off a retinal vessel by moving the fixation target carefully.

The first experiment was performed to investigate the integration effect by varying the gate time T_g. Figure 6 shows typical correlation functions measured with $\Delta\tau=1$ μs ($p=1$), together with direct plots of the integrated count data m for three different values of the gate time which were obtained from a retinal vessel (a) and a surrounding tissue area (b). Each measurement was made for 2.1 s with the sampling time $t_s=1$ μs. The correlation functions in (a) and (b) demonstrate a clear difference with about four times in the correlation time. The difference is found in the direct plots between the vessel and tissue with a short gate time of $T_g=16$ μs. However, it is not large enough to discriminate safely data for the vessel from those for the tissue, since the integration effect in the sequential count data is less remarkable with $T_g=16$ μs (which is too short). The difference is enhanced with a longer gate time, consequently the direct plots being smoothed out. A difference in the signal fluctuations between (a) and (b) is noticeable in the case of a longer gate time as expected. We, then, measured the specific variance of pulse counts obtained from a retinal vessel and a surrounding tissue area. Most of the data were distributed in regions of $\sigma^2/\langle m\rangle<10$ for the vessel and $\sigma^2/\langle m\rangle>10$ for the tissue with a good separation. This indicates that the data discrimination with the specific variance is likely to be possible for *in vivo* measurements.

The next experiment was carried out to verify the ability of eliminating the effect of actual eye movements on human retina. To increase intentionally the probability of eye-movement occurrence during a measurement, one measurement period was expanded to be 6.3 s for which all the photon count data were sequentially stored in a memory with a 1 μs sampling time. Figure 7 shows temporal recordings of the specific variance obtained with the 2.048 ms gate time and the 65.5 ms unit time and corresponding correlation functions with $\Delta\tau=1$ μs ($p=1$) for two types of the displacement (I) from

the vessel to the tissue and (II) from the tissue to the vessel. The specific variance $\sigma^2/\langle m\rangle$ takes a large value in the latter part of the result (I) and in the first part of the result (II) where we visually observed that the measuring point was located off a vessel. This means that the specific variance gives a useful criterion for specifying what part of the stored data comes from the vessel or the tissue. The correlation functions in (b) and (c) were calculated from all of the data in the period "**A**" and from the part of the data in the selected period "**V**", respectively. The correlation functions in (b) have a quite slow decay which corresponds to a long-term tail component caused by the low frequency fluctuation of bio-speckles from the tissue. This is undesirable for estimating a correlation time. The correlation functions in (c) show an early-decaying curve which we expect for the blood flow. This is due to the elimination of erroneous data coming from the surrounding tissue area which show a large specific variance. The specific variance of $\sigma^2/\langle m\rangle = 6$ was used for a criterion of the elimination in (c). Therefore, the retinal blood flow can be successfully evaluated from a part of the sequential count data even if the measuring point is displaced by eye movements during a measurement.

As described in Sec. 3.1, the present signal-analyzing system has the function of time-division correlation analysis. Then, we further investigated the case of Figure 7(II) as an example by using this function, and compared the results with those of Figure 7(II). After reading out the raw sequential count data of Figure 7(II) from the memory, we divided them into 12 subperiods, each of which has the 525 ms length, and calculated the correlation function with the delay time unit $\Delta\tau = 1\ \mu$s ($p = 1$) for each. Figure 8 shows twelve correlation functions obtained in such a way. The first three correlation functions demonstrate a relatively slow decay while other functions after the three attenuate rapidly. The temporal variation of the reciprocal of correlation time, $1/\tau_c$, was also obtained from the correlation functions of Figure 8. The $1/\tau_c$ value was small in the beginning and, then, increased after 1.5 s. This variation agreed well with the temporal change of the specific variance in (a) of Figure 7(II), although the two values have roughly a reciprocal relation from each other. This means that the direct analysis of time-division correlation functions is also able to discriminate the data for the retinal vessel from those for the tissue. However, the estimation using the specific variance has much better temporal resolution (about two orders) with a smaller calculating time and, therefore, it is more advantageous than that of the time-division correlation analysis. A problem of the specific variance may be that it is rather sensitive to noises, as is easily observed from many local minima and maxima in the results of Figures 7(I)-(a) and 7(II)-(b).

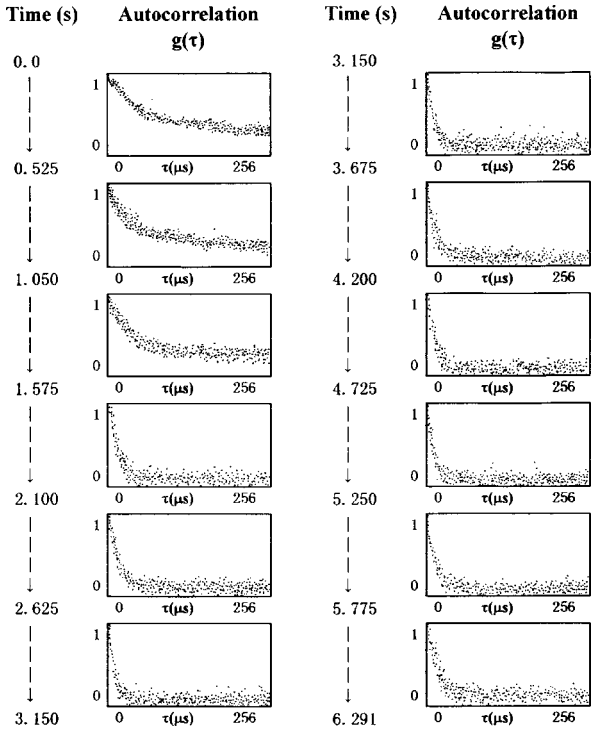

Fig. 8 Variation of correlation functions when the measuring point was moving into the retinal vessel from the tissue.

5 CONCLUSION

The flexible correlation-analyzing method was described on the basis of the photon correlation technique. The system has the following "flexible" characteristics which enable us to extract effectively the retinal blood flow information from erroneous data: (1) variable sampling time, (2) variable delay time unit, (3) count data storing and repeatable analysis, (4) time-division analysis, (5) erroneous data discrimination and rejection.

Thus, the proposed system is expected to reduce the effects of eye-movement artifacts and other various external moving factors. The continuing *in vivo* experiments are necessary for establishing the usefulness of this technique for various clinical situations. However, one should carefully treat the item (5), because the discrimination assumes a clear difference in the correlation times for the retinal vessel and for the surrounding tissue, with usually four times or larger. This operation may possibly be ineffective for some of diseased eyes in which speckle fluctuations in the retinal vessel and the surrounding tissue area are close to each other in a correlation time. In this case, an alternative discrimination method such as reflectance spectroscopy should be developed.

REFERENCES

1. Y. Aizu and T. Asakura, "Bio-speckle phenomena and their application to the evaluation of blood flow," *Opt. Laser Technol.* **23**, 205–219 (1991).
2. K. D. Hinsch, "Optical methods in bioindication," in *Optics*

for Protection of Man and Environment against Natural and Technological Disasters, G. von Bally and H. I. Bjelkhagen, Eds., pp. 267-278, Elsevier Science, Amsterdam (1993).
3. Z. Xu, C. Joenathan, and B. M. Khorana, ''Temporal and spatial properties of the time-varying speckles of botanical specimens,'' *Opt. Eng.* **34**, 1487–1502 (1995).
4. J. D. Briers, ''Monitoring biomedical motion and flow by means of coherent light fluctuations,'' *Proc. SPIE* **2732**, 2–15 (1996).
5. B. M. Khorana, ''Lasers in diagnostic dentistry,'' *Proc. SPIE* **2887**, 7–12 (1996).
6. J. A. Cole and M. H. Tinker, ''Laser speckle spectroscopy—a new method for using small swimming organisms as biomonitors,'' *Bioimaging* **4**, 243–253 (1996).
7. Y. Aizu and T. Asakura, ''Bio-speckles,'' in *Trends in Optics*, A. Consortini, Ed., pp. 27–49, Academic, London (1996), and references therein.
8. Y. Aizu, K. Ogino, T. Sugita, T. Yamamoto, N. Takai, and T. Asakura, ''Evaluation of blood flow at ocular fundus by using laser speckle,'' *Appl. Opt.* **31**, 3020–3029 (1992).
9. Y. Aizu, T. Asakura, K. Ogino, T. Sugita, Y. Suzuki, and K. Masuda, ''Bio-speckle flowmetry for retinal blood flow diagnostics,'' *Bioimaging* **4**, 254–267 (1996).
10. R. W. Ditchburn, ''Eye-movements in relation to retinal action,'' *Opt. Acta* **1**, 171–176 (1955).
11. R. W. Ditchburn, ''A new apparatus for producing a stabilized retinal image,'' *Opt. Acta* **10**, 325–331 (1963).
12. C. E. Riva and B. L. Petrig, ''Retinal blood flow: laser Doppler velocimetry and blue field simulation technique,'' in *Noninvasive Diagnostic Techniques in Ophthalmology*, B. R. Masters, Ed., pp. 390–409, Springer-Verlag, New York (1990), and references therein.
13. M. T. Milbocker, G. T. Feke, and D. G. Goger, ''Laser Doppler velocimetry stabilized in one dimension,'' *IEEE Trans. Biomed. Eng.* **38**, 928–930 (1991).
14. M. J. Mendel, V. V. Toi, C. E. Riva, and B. L. Petrig, ''Laser Doppler velocimeter stabilized in two dimensions,'' *Invest. Ophthalmol. Vis. Sci. Suppl.* **33**, 807 (1992).
15. M. J. Mendel, V. V. Toi, C. E. Riva, and B. L. Petrig, ''Eye-tracking laser Doppler velocimeter stabilized in two dimensions: principle, design, and construction,'' *J. Opt. Soc. Am. A* **10**, 1663–1669 (1993).
16. Y. Aizu, H. Ambar, T. Yamamoto, and T. Asakura, ''Measurements of flow velocity in a microscopic region using dynamic laser speckles based on the photon correlation,'' *Opt. Commun.* **72**, 269–273 (1989).
17. Y. Aizu, A. Kojima, M. Suematsu, and T. Asakura, ''Signal analysis for retinal blood-flow measurements using biospeckle phenomena,'' in *Optical Methods in Biomedical and Environmental Sciences*, H. Ohzu and S. Komatsu, Eds., pp. 159–162, Elsevier Science, Amsterdam (1994).
18. Hamamatsu Photonics Technical Data, Photon Counting (February, 1992).
19. R. G. W. Brown, K. D. Ridley, and J. G. Rarity, ''Characterization of silicon avalanche photodiodes for photon correlation measurements. 1: Passive quenching,'' *Appl. Opt.* **25**, 4122–4126 (1986).
20. *Photon Correlation and Light Beating Spectroscopy*, H. Z. Cummins and P. R. Pike, Eds., Plenum, New York (1973).
21. L. E. Drain, *The Laser Doppler Technique*, Wiley, New York (1980).
22. A. Papoulis, *Probability, Random Variables, and Stochastic Processes*, 2nd ed., McGraw–Hill, Singapore (1984).
23. J. Ohtsubo and T. Asakura, ''Velocity measurement of a diffuse object by using time-varying speckles,'' *Opt. Quantum Electron.* **8**, 523–529 (1976).
24. J. W. Goodman, ''Statistical properties of laser speckle patterns,'' in *Laser Speckle and Related Phenomena*, J. C. Dainty, Ed., pp. 9–75, Springer-Verlag, Berlin (1984).